

# Hydrodynamic Lubrication Using Non-Newtonian Fluid for Journal Bearing and Multi Lobe Bearing

Ishanka Saikia Linturoy\*

Assistant Professor ,NIT Silchar

Date of Submission: 20-11-2023

Date of Acceptance: 30-11-2023

**ABSTRACT:** This paper presents the performance characteristics for dilatant lubricant having flow behaviour index (n) 1.4,1.5,...,2.1. To find the steady state performance characteristics two axial groove and multi lobe hydrodynamic bearing and check how greatly these values vary with different values of eccentricity ratio and flow behaviour index. For many bearings to function at high speeds under heavy loads, lubricants based on mineral oils with high molecular weight polymers have become increasingly popular. These lubricants due to the presence of different types of additives behave like non-Newtonian fluids. This addition of additives improve the viscosity index of the oil and nominal load capacity of the bearing . Technology advancements and stringent machine operational requirements demanded the development of better lubricants to ensure smooth and safe operation. From this paper an effort is taken to find the extent of power law index up to which dilatancy exists, viscosity index

**keywords;** non-Newtonian fluids, flow behaviour index, additives, multi lobe hydrodynamic, dilatant lubricant

## I. INTRODUCTION:

The requirement for many bearings to operate at high speed under heavy loads has led to the increasing use of lubricant consisting of mineral oils to which polymers of high molecular weight have been added. These lubricants due to the presence of different types of additives. behave like non-Newtonian fluids. According to P.D. William [31], this addition of additives improve the viscosity index of the oil and nominal load capacity of the bearing. Advancement in technology and severe operational requirements of machines necessitated the development of improved lubricants for smooth and safe operation. Dean and Davis [32] introduced

the notion of the Viscosity Index (VI) in 1929, and it was discovered that viscosity varies with temperature. For operations under high speeds any heavy loads, oils containing high molecular weight polymers as viscosity index improvers are used to prevent viscosity variation with temperature. The increase in temperature causes the kinetic or thermal energy to increase and the molecules become more mobile. The attractive binding energy is reduced and therefore viscosity is reduced. Using various non-Newtonian lubricants, the performance characteristics of hydrodynamic bearings can be improved to the desired machine requirements. Currently, ethylene and propylene-based olefin copolymer are widely used as viscosity index improver [33].

Oliver [34] conducted an experiment for short bearing with lubricants containing polymer additives and found that there was an improvement in load carrying capacity whereas a reduction in friction was observed. Similarly, to analyse the effect of granular additives on hydrodynamic lubrication, Dai and Khonsari [35, 36] developed an alternate approach based on continuum approach and theory of mixture.

This theoretical study reveals improvement in load- carrying capacity and reduction in friction. In 1974, Maiti [37] used a micro-polar model to explore the squeeze film effects between circular plates separated by lubricants containing solid additives and found that load carrying capacity rises when compared to Newtonian lubricant. Khonsari and Brewe [38] conducted a theoretical investigation of bearing performance characteristics of finite journal bearings working with micro-polar lubricants and found that there is a significant increase in load-carrying capacity and reduction in friction coefficient when compared to Newtonian lubricants.

Hsu [39] used the cubic shear stress law for the non-Newtonian lubricants and studied the static performance characteristics for infinitely long bearings by expressing pressure and flow in terms of power series. Swamy et. al. [40-42] solved the modified Reynolds equation using the cubic shear stress vs shear strain rate law and studied the performance characteristics for finite-width bearings. Later, Tayal et. al. [43] solved the Navier-Stokes equations by the finite element method and used the cubic shear stress law for non-Newtonian lubricants to study the static performance characteristics for an infinitely long bearing. Ashutosh Kumar et. al. [44] studied the effect of couple stress parameter on the steady-state performance characteristics of two-lobe bearing operating with non-Newtonian fluid and found that the couple stress parameter enhances the load-carrying capacity and it also reduces the friction variable. Until now, many dilatant fluids have been found such as Oobleck (Cornflour and water mixture), China Clay, and Titanium Dioxide whose value of  $n$  is more than one and there might be a good future scope of finding many other efficient dilatant lubricants. Some obtained numerical results also show that for dilatant fluid ( $n > 1$ ), the load-carrying capacity increases while in pseudo-plastics ( $n < 1$ ) it decreases [45]. Due to this study of these dilatant fluids as lubricant in hydrodynamic bearing becomes very essential. In this paper focus will be concentrated on finding the performance characteristics such as load-carrying capacity, Friction variable, Attitude angle and Flow coefficient for dilatant lubricant and to get an idea about how changing the value of  $n$  effect on the performance characteristics of the hydrodynamic journal bearing. In this study, how these

performance characteristics greatly vary with changing the value  $n$  from 1.4 to 2.1 will be studied.

**Theory:** The Reynolds equation for Newtonian incompressible and constant viscosity fluid is given by

$$\frac{\partial}{\partial x} \left( \frac{h^3}{\eta_L} \frac{\partial p}{\partial x} \right) + \frac{\partial}{\partial z} \left( \frac{h^3}{\eta_L} \frac{\partial p}{\partial z} \right) = 6U \frac{\partial h}{\partial x} \dots \dots \dots (1)$$

Dien and Elrod derived the modified Reynolds' equation for finite journal bearing using power-law fluids and the basic assumptions in the theory of hydrodynamic lubrication. The simplified form of Reynolds equation for non-Newtonian fluid can be written as [2]

$$\frac{\partial}{\partial x} \left( \frac{h^{2+n}}{\eta_L} \frac{\partial p}{\partial x} \right) + \frac{\partial}{\partial z} \left( \frac{h^{2+n}}{\eta_L} \frac{\partial p}{\partial z} \right) = 6U^n \frac{\partial h}{\partial x} \dots \dots \dots (2)$$

Various non-dimensional terms used in Reynolds equations are as follows

$$\bar{p} = \frac{pc^2}{6\eta v R} \bar{h} = \frac{h}{c}, \quad \varepsilon = \frac{e}{c} \quad \theta = \frac{x}{R}, \quad \bar{y} = \frac{y}{h}, \quad \bar{z} = \frac{z}{(L/2)}$$

The Reynolds equation is solved by Finite Difference Method. All the differentials in the equation are to be replaced by finite difference approximations.

A developed view of half of the bearing is drawn as shown in Fig. 1. The area is divided into a number of mesh size ( $\Delta\theta, \Delta\bar{z}$ ). The area is divided into  $U$  equal parts of lengths of  $\Delta\theta$  and the total is equal to  $2\pi$  such that  $\Delta\theta = 2\pi/U$

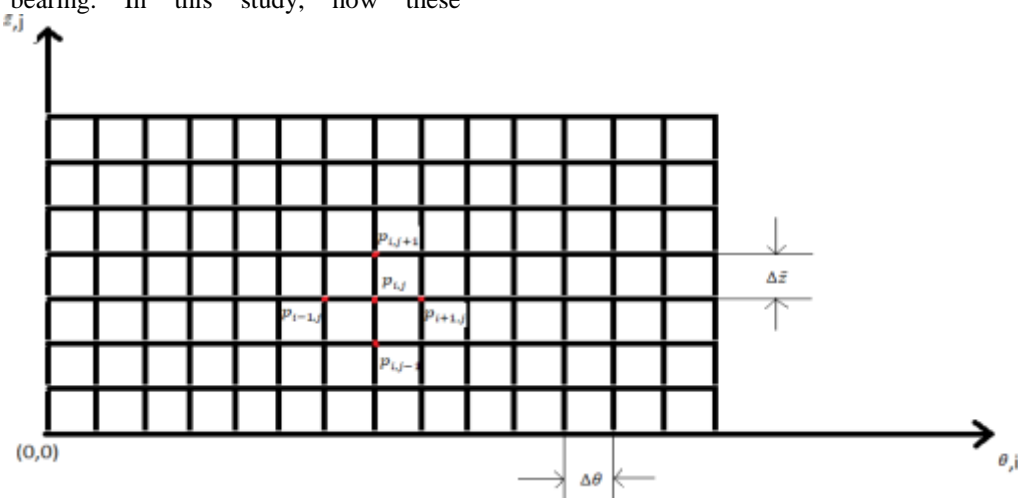


FIGURE 1 A developed view of a bearing showing the mesh size ( $\Delta\theta, \Delta\bar{z}$ )

The finite difference approximations that are used can be written as follows

$$\frac{\partial^2 \bar{p}}{\partial \theta^2} = \frac{\bar{p}_{i+1,j} - 2\bar{p}_{i,j} + \bar{p}_{i-1,j}}{(\Delta\theta)^2}, \quad \frac{\partial^2 \bar{p}}{\partial z^2} = \frac{\bar{p}_{i,j+1} - 2\bar{p}_{i,j} + \bar{p}_{i,j-1}}{(\Delta z)^2}$$

$$\frac{\partial \bar{p}}{\partial \theta} = \frac{\bar{p}_{i,j+1} - \bar{p}_{i,j-1}}{2\Delta\theta}, \quad \frac{\partial \bar{p}}{\partial z} = \frac{\bar{p}_{i+1,j} - \bar{p}_{i-1,j}}{2\Delta z}$$

Where,  $p_{i,j}$  is the pressure at any mesh point (i, j)

$p_{i+1,j}; p_{i-1,j}; p_{i,j+1}; p_{i,j-1}$  are four adjacent points.

(i, j) is the numerical co-ordinate system.

Now pressure at any mesh point (i, j) is expressed in terms of pressure of four adjacent points

$$p_{i,j} = \frac{1}{2 \left( 1 + \left( \frac{D}{L} \right)^2 \left( \frac{\Delta\theta}{\Delta z} \right)^2 \right)} \left[ (\bar{p}_{i+1,j} + \bar{p}_{i-1,j}) + \left( \frac{3}{2} \right) \left( \frac{\epsilon \sin \theta (\Delta\theta)}{h} \right) (\bar{p}_{i+1,j} - \bar{p}_{i-1,j}) + \left( \frac{D}{L} \right)^2 \left( \frac{\Delta\theta}{\Delta z} \right)^2 (\bar{p}_{i,j+1} + \bar{p}_{i,j-1}) + \frac{\epsilon \sin \theta (\Delta\theta)^2}{(\bar{h})^3} \right]$$

The convergence criterion adopted for pressure calculation is

$$\left| 1 - \frac{\sum \bar{p}_{old}}{\sum \bar{p}_{new}} \right| \leq 10^{-5}$$

Various performance characteristics are calculated as follows.

### Load Calculation

Load carrying capacity can be calculated by the following component of force along perpendicular to the line of centre

$$\bar{W}_x = \int_0^{2\pi} \bar{p} \cos\theta \cdot d\theta \dots \dots \dots (3)$$

$$\bar{W}_y = \int_0^{2\pi} \bar{p} \sin\theta \cdot d\theta \dots \dots \dots (4)$$

Therefore load carrying capacity of the journal bearing is given by

$$\bar{W} = \sqrt{(\bar{W}_x)^2 + (\bar{W}_z)^2} \dots \dots \dots (5)$$

$$\bar{W} = \frac{c^2 W}{6\eta R^2 U L}$$

The attitude angle is given by the term

$$\phi = \tan^{-1} \left( \frac{\bar{W}_z}{\bar{W}_x} \right)$$

### Flow Calculation

The non-dimension flow coefficient can be calculated by the equation [6] given in

$$\bar{q}_z = \frac{1}{2} \left( \frac{D}{L} \right)^2 \int_0^{2\pi} \bar{h}^3 \frac{\partial \bar{p}}{\partial z} d\theta \dots \dots \dots (6)$$

### Friction force calculation

Friction force in contact surface is given by

$$F_z = \int_0^{2\pi} \tau_z LR \cdot d\theta$$

Where  $\tau_z$  is the shear stress on journal surface and it is given by

$$\tau_z = \frac{\eta U}{\bar{h}c} + \frac{\bar{h}c}{2R} \frac{6\eta RU}{c^2} \frac{\partial \bar{p}}{\partial \theta}$$

Non dimensional form of friction force

$$\bar{F}_z = LR \int_0^{2\pi} \left( \frac{\eta U}{\bar{h}c} + \frac{3\eta U \bar{h}}{c} \frac{\partial \bar{p}}{\partial \theta} \right) d\theta$$

Friction co-efficient

$$\mu = \frac{\bar{F}_z}{W} = \frac{\int_0^{2\pi} \left( \frac{\eta U}{hc} + \frac{3\eta U h}{c} \frac{\partial p}{\partial \theta} \right) d\theta}{\frac{6\eta U R^2 L W}{c^2}}$$

The friction variable is given by

$$\bar{\mu} = \frac{\bar{F}}{W} = \frac{\int_0^{2\pi} \left( \frac{1}{h} + 3h \frac{\partial p}{\partial \theta} \right) d\theta}{6W} \dots\dots\dots(7)$$

**Sommerfeld no**

$$S = \frac{\eta N}{P} \left( \frac{R}{C} \right)^2, \quad \text{Where, } P = \frac{W}{2LR}$$

$$\text{In non dimensional form } S = \frac{1}{6\pi W}$$

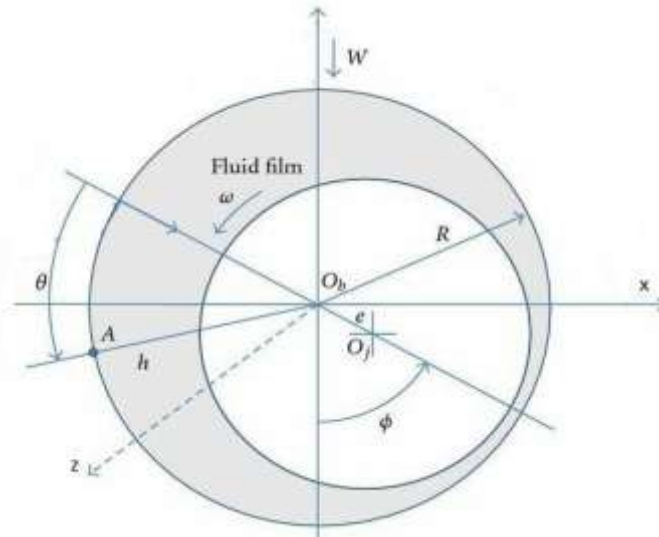


**FIGURE 2** Plain Cylindrical bearing

**Mathematical Modelling**  
**TWO AXIAL GROOVE BEARING**

In two axial groove bearing, the grooves are located at horizontal position at 180° apart as shown in figure 3. The lubricant is fed from groove having groove angle (α<sub>g</sub>) 20° and groove length (G<sub>L</sub>) is equal to total length of bearing. The fluid film is generated at the land region due to hydrodynamic action. The flow in this region will be both circumferential and axial. The lubricants flow out from the bearing ends axially. The

pressure generated due to the wedge action in the clearance space supports the load without metal to metal contact.

Once the pressure distribution is obtained using various different boundary conditions, by using Simpson one third numerical integration method non-dimensional load is calculated. After finding the load capacity Sommerfeld number, Attitude angle, friction variable and flow coefficients are calculated.

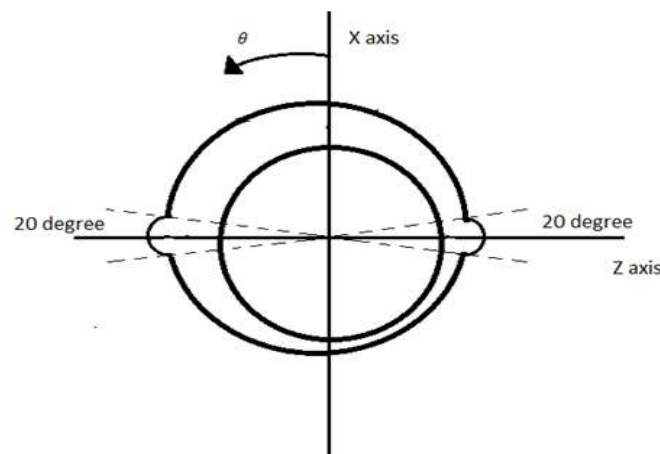


**FIGURE 3** :Cross section of two axial groove bearing [49]

### Two Lobe Bearing

The Fig. 10 shows the schematic diagram of two-lobe bearing.  $O_1$  and  $O_2$  are the centres of lobe 1 and lobe 2. Although each lobe of the bearing is circular, but the geometric configuration

of the bearing is not circular. In present work two lobes of 160 degree are separated by two axial grooves of 20 degree extensions in horizontal direction. The distance between centre and the centre of individual lobe

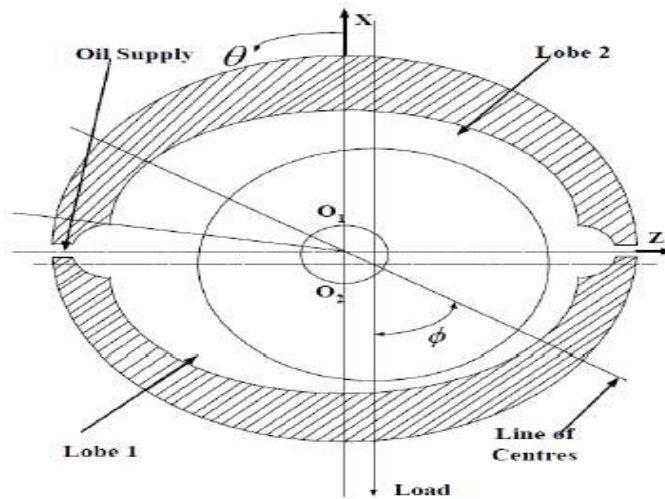


FIGURE 10 Two-lobe Journal bearing

is known as ellipticity ( $e_p$ ) and ellipticity ratio ( $\delta$ )

is defined as  $\frac{e_p}{\delta}$ .

From geometry, eccentricity ratios of individual lobes are given as:

$$\epsilon_1 = \sqrt{\epsilon^2 + \delta^2 + 2\epsilon\delta\cos\theta} \quad (8)$$

$$\epsilon_2 = \sqrt{\epsilon^2 + \delta^2 - 2\epsilon\delta\cos\theta} \quad (9)$$

Similarly, attitude angle of individual lobe is given as:

$$\phi_1 = \tan^{-1} \frac{e \sin \phi}{d + e \cos \phi}$$

Where  $\epsilon_2 = \frac{e_2}{c}$  is the eccentricity ratio

of lobe 2.

$$\text{Also } \phi_2 = \pi - \tan^{-1} \frac{\epsilon \sin \phi}{\delta - \epsilon \cos \phi}$$

### Three Lobe Bearing

The bearing as shown in Fig. 3.5 consists of three lobes. Each lobe of the bearing is circular, but the geometric configuration of the bearing is not. The centre of each lobe displaced an equal distance called ellipticity, from the centre of the bearing.

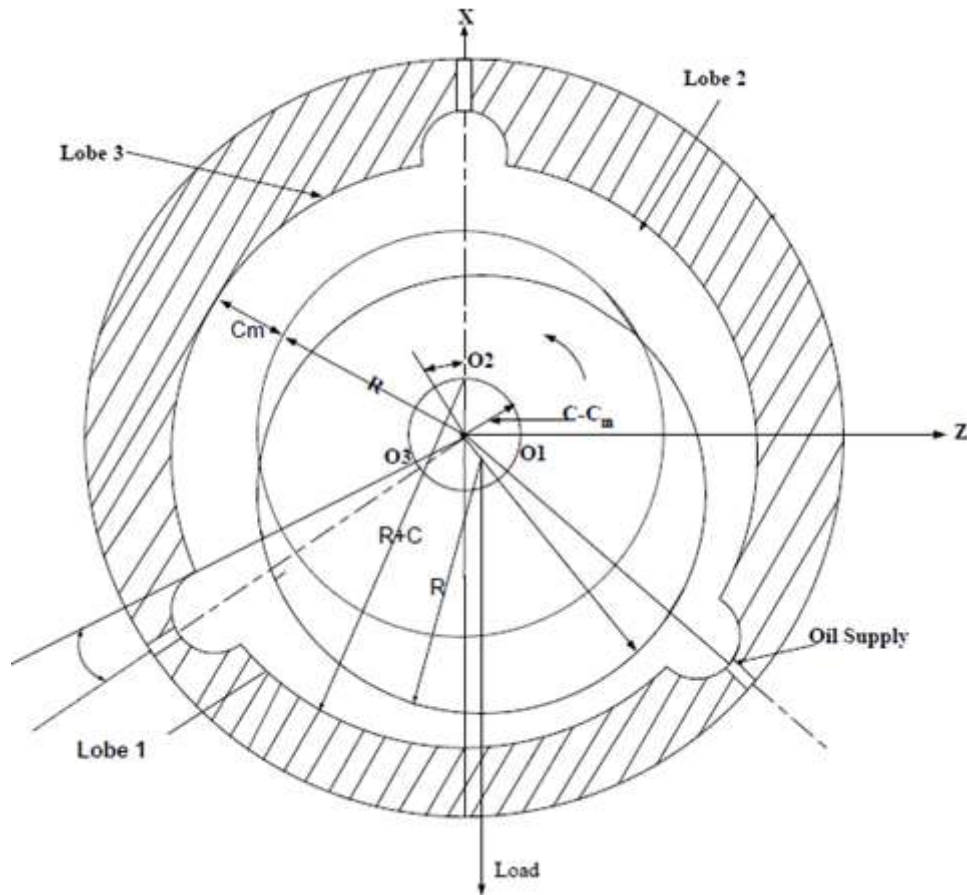


FIGURE 11. Three-lobe Bearing

For lobe 1

$$\varepsilon_1 = \sqrt{\varepsilon^2 + \delta^2 + 2\varepsilon\delta \cos\phi} \quad (10)$$

$$\phi_1 = \tan^{-1} \frac{e \sin \phi}{d + e \cos \phi} \quad (11)$$

For lobe 2

$$\varepsilon_2 = \sqrt{\varepsilon^2 + \delta^2 - 2\varepsilon\delta \cos\left(\frac{\pi}{3} + \phi\right)} \quad (12)$$

$$\phi_2 = \frac{2\pi}{3} - \tan^{-1} \frac{\varepsilon \sin\left(\frac{\pi}{3} + \phi\right)}{\delta - \varepsilon \cos\left(\frac{\pi}{3} + \phi\right)} \quad (13)$$

For lobe 3

$$\varepsilon_3 = \sqrt{\varepsilon^2 + \delta^2 - 2\varepsilon\delta \cos\left(\frac{\pi}{3} - \phi\right)} \quad (14)$$

$$\phi_3 = \frac{2\pi}{3} - \tan^{-1} \frac{\varepsilon \sin\left(\frac{\pi}{3} - \phi\right)}{\delta - \varepsilon \cos\left(\frac{\pi}{3} - \phi\right)} \quad (15)$$

#### FOUR LOBE BEARING

12. shown in figure consists of four lobes. Here, the maximum span of a lobe is 90 degree. However, the lobes are separated by axial grooves for allowing the oil and in this work 20 degree grooves are considered. Therefore, the net span of For lobe 1,

For lobe 1

$$\varepsilon_1 = \sqrt{\varepsilon^2 + \delta^2 + 2\varepsilon\delta \cos\phi} \quad (16)$$

$$\phi_1 = \tan^{-1} \frac{\varepsilon \sin\phi}{\delta + \varepsilon \cos\phi} \quad (17)$$

For lobe 2

$$\varepsilon_2 = \sqrt{\varepsilon^2 + \delta^2 - 2\varepsilon\delta \cos\left(\frac{\pi}{2} + \phi\right)} \quad (18)$$

$$\phi_2 = \frac{\pi}{2} - \tan^{-1} \frac{\varepsilon \sin\left(\frac{\pi}{2} + \phi\right)}{\delta - \varepsilon \cos\left(\frac{\pi}{2} + \phi\right)}$$

For lobe 3

$$\varepsilon_3 = \sqrt{\varepsilon^2 + \delta^2 - 2\varepsilon\delta \cos\phi} \quad (19)$$

$$\phi_3 = \pi - \tan^{-1} \frac{\varepsilon \sin\phi}{\delta - \varepsilon \cos\phi} \quad (20)$$

For lobe 4

$$\varepsilon_4 = \sqrt{\varepsilon^2 + \delta^2 - 2\varepsilon\delta \cos\left(\frac{\pi}{2} - \phi\right)} \quad (21)$$

$$\phi_4 = \frac{\pi}{2} - \tan^{-1} \frac{\varepsilon \cos\phi}{\delta - \varepsilon \sin\phi} \quad (22)$$

For lobe 3

$$\varepsilon_3 = \sqrt{\varepsilon^2 + \delta^2 - 2\varepsilon\delta \cos\phi} \quad (23)$$

$$\phi_3 = \pi - \tan^{-1} \frac{\varepsilon \sin\phi}{\delta - \varepsilon \cos\phi} \quad (24)$$

For lobe 4

$$\varepsilon_4 = \sqrt{\varepsilon^2 + \delta^2 - 2\varepsilon\delta \cos\left(\frac{\pi}{2} - \phi\right)}$$

each lobe is 70 degree. The individual lobe eccentricities ( $\varepsilon_1, \varepsilon_2, \varepsilon_3, \varepsilon_4$ ) and attitude angle ( $\phi_1, \phi_2, \phi_3, \phi_4$ ) are related to the bearing eccentricity. These relationships are presented in equation 3.20 to equation 3.27 are obtained from the geometry of the two lobe bearing

(25)

$$\phi_4 = \frac{\pi}{2} - \tan^{-1} \frac{\varepsilon \cos \phi}{\delta - \varepsilon \sin \phi} \quad (26)$$

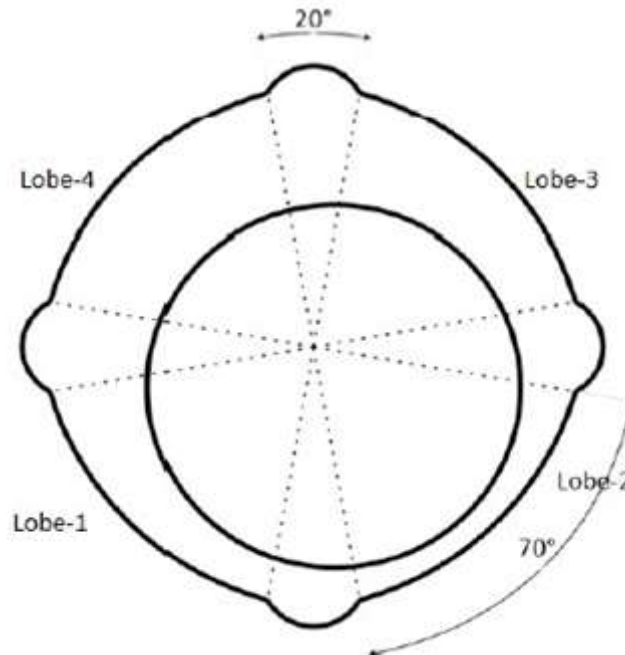


FIGURE 12 Four-Lobe Bearing

**RESULTS Plain Cylindrical Bearing :** The values of steady-state performance characteristics for plain cylindrical bearing, two axial groove bearing and two lobe bearing are obtained by using Numerical solution of Reynolds equation has presented. The steady state performance characteristics are obtained for non-Newtonian lubricant having flow behaviour index  $n=1.4, 1.5, 1.6, 1.7, 1.8, 1.9, 2$  and  $2.1$  as well as for Newtonian lubricant.

**Estimation of Steady State Performance Characteristics of Plain Cylindrical Bearing Using Non-Newtonian Fluid (Dilatant Fluid from  $n=1.4$  to  $2.1$ )**

Using numerical solution of Reynolds equation, Steady State performance characteristics are calculated for power-law index,  $n=1.4, 1.5, 1.6, 1.7, 1.8, 1.9, 2$  and  $2.1$  for plain cylindrical bearing as shown in Table 1 and the  $L/D$  ratio considered here is 1. Following results are the observations noted

TABLE 1 For  $L/D=1, n=1$  validation of theoretical model for plain cylindrical bearing

$\epsilon$	S [47]	$\phi$ [47]
0.1	1.3299 [1.3500]	79.4073 [79]
0.2	0.6318 [0.6320]	73.8573 [74]
0.3	0.3888 [0.3820]	68.2595 [68]
0.4	0.2604 [0.2610]	62.5604 [62]
0.5	0.1786 [0.1790]	56.6940 [56]
0.6	0.1209 [0.1200]	50.5162 [50]
0.7	0.0777 [0.0765]	43.8111 [43]
0.8	0.0445 [0.0448]	36.1657 [36]
0.9	0.0187 [0.0191]	26.3309 [25]



As shown in Fig.13 for all power-law index values from  $n=1.4$  to  $2.1$ , the value of attitude angle decreases while increasing the values of eccentricity ratio. Similarly, for a particular eccentricity ratio, the attitude angle decreases while increasing the values of flow behaviour index from  $1.4$  to  $2.1$ .

On the other hand, for all power law index values from  $n=1.4$  to  $2.1$ , the value of Load Carrying Capacity increases while increasing the values of eccentricity ratio as shown in Fig. 14. In addition, while keeping the eccentricity ratio constant, the values of Load Carrying Capacity increase while increasing the values of flow behavior index  $1.4$  to  $2.1$ . On increasing the value of  $n$  and  $\epsilon$  the pressure increases inside the bearing. The values of Sommerfeld Numbers can be observed decreasing while increasing the eccentricity ratio values keeping the value of flow behaviour index constant as shown in Fig.15 At a

given value of eccentricity ratio, the value of friction variable decreases while increasing the flow behaviour index from  $1.4$  to  $2.1$  as shown in Fig. 17. Similarly, at a given value of power law index, the values of Friction Variable decrease while keeping the value of eccentricity ratio constant. Due to increase of lubricant pressure, it is clear that the fluid film thickness reduces. Thus friction variable, which is directly proportional to fluid film thickness, will also reduce.

With the increase of power law index from  $1.4$  to  $2.1$ , the values of flow coefficient increases for same value of eccentricity ratio as shown in Fig. 17. On keeping the power law index constant, on increasing the values of eccentricity ratio the value of Flow Coefficient increase. Flow coefficient is directly proportional to pressure. As the value of pressure inside the lubricant increases on increasing  $n$  and  $\epsilon$ , thus the value of flow coefficient also increases.

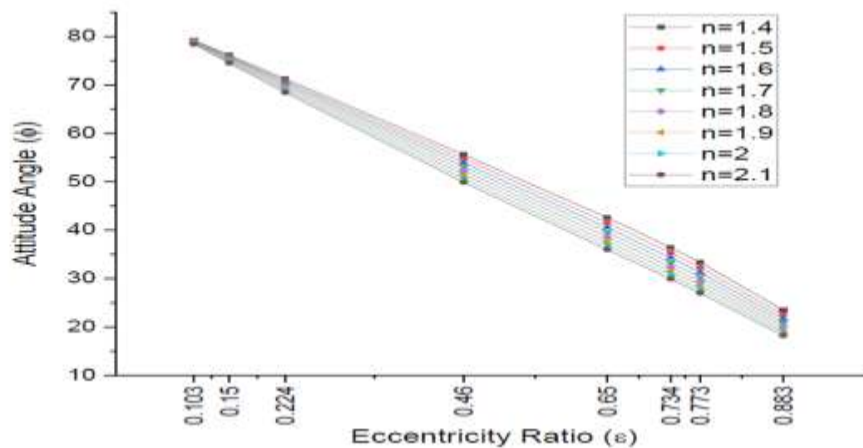


FIGURE 13 Variation of Attitude Angle with eccentricity ratio & power law index

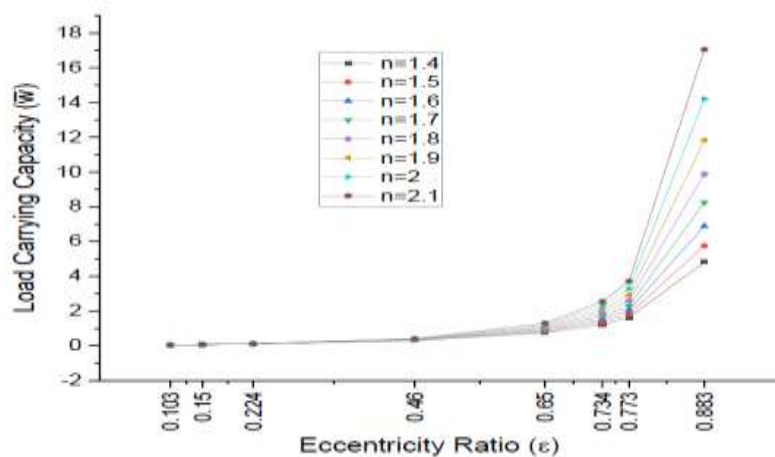


FIGURE 14 Variation of Load Capacity with eccentricity ratio & power la

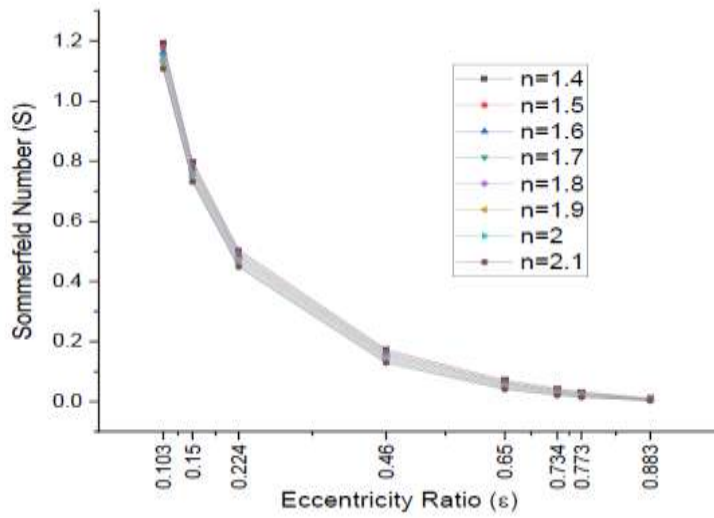


FIGURE 15 Variation of Sommerfeld No. with eccentricity ratio & power law index

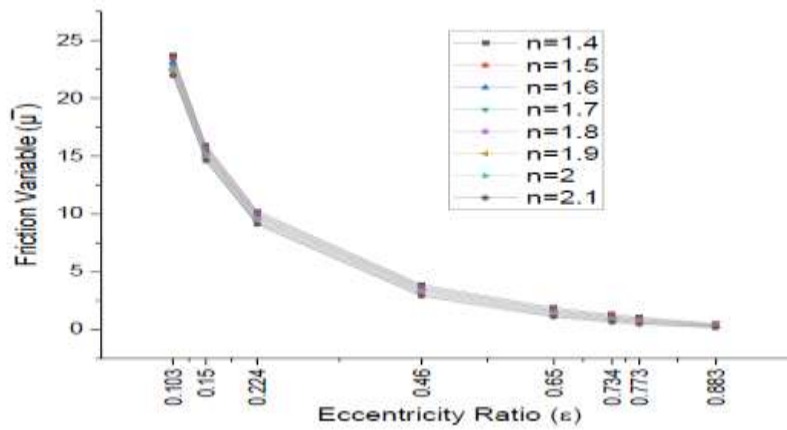


FIGURE 16 Variation of Friction Variable with eccentricity ratio & power law index

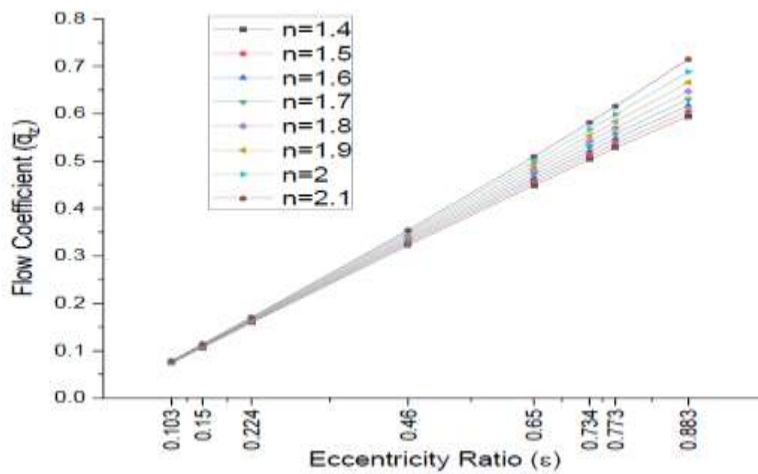


FIGURE 17 Variation of Flow Coefficient with eccentricity ratio & power law index

### Two Axial Groove Bearing

In two axial groove bearing, the grooves are located at horizontal position at 180 degrees apart, as shown in Fig. 18. The lubricant is fed from groove having groove angle 20 degree and groove length equal to total length of the bearing. The fluid film is generated at the land region due to hydrodynamic action. The flow in this region will be both circumferential and axial. The lubricants flow out from the bearing ends axially. The pressure generated due to the wedge action in the

clearance space supports the load without metal-to-metal contact.

Once the pressure distribution is obtained using various different boundary conditions, by using Simpson one third numerical integration method non-dimensional load is calculated. After finding the load capacity Sommerfeld number, Attitude angle, friction variable and flow coefficients are calculated.

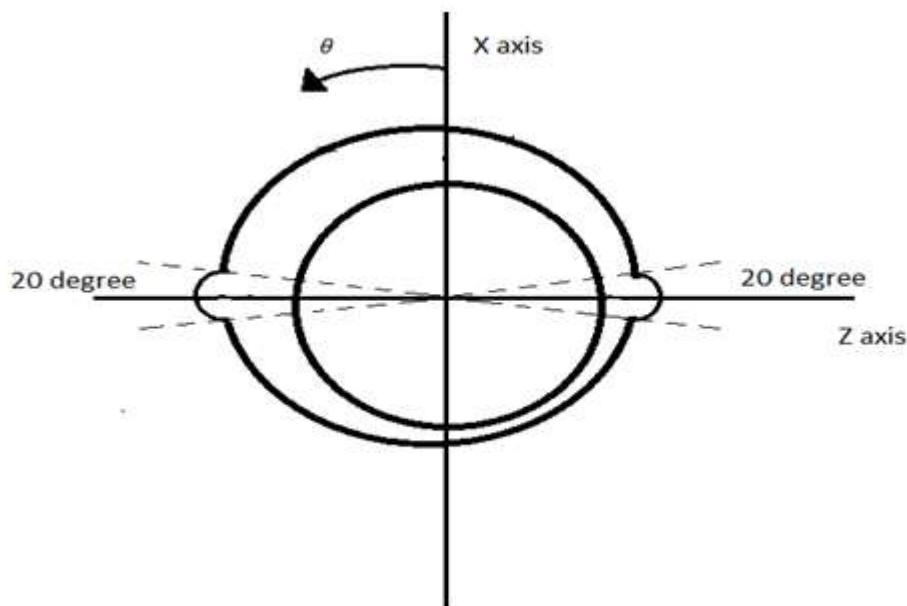


FIGURE 18 Cross section of two axial groove bearing [49]

Table 2 shows the steady state performance characteristics “S” and “ $\phi$ ” are obtained for Two Axial Groove bearing. These values are compared with previously published Lund W., Thomson K.

K., “A calculation method and Data for the dynamic coefficients of oil lubricated journal bearings”, 1978 [48]

TABLE 2 For L/D=1, n=1 validation of theoretical model for two axial groove bearing

$\epsilon$	S [48]	$\phi$ [48]
0.103	1.4782 [1.4700]	73.7900 [75.9900]
0.150	1.0036 [0.9910]	68.1600 [71.5800]
0.224	0.6461 [0.6350]	61.9475 [63.5400]
0.460	0.2386 [0.2350]	48.9475 [49.2700]
0.650	0.1091 [0.1080]	39.4225 [39.7200]
0.734	0.0717 [0.0710]	34.8950 [35.1600]
0.773	0.0571 [0.0560]	32.5800 [32.8600]
0.883	0.0238 [0.0240]	24.7600 [25.0200]

### Estimation of Steady State Performance Characteristics of Two Axial Groove Bearing Using Non-Newtonian Fluid (Dilatant Fluid from n=1.4 to 2.1)

Using numerical solution of Reynolds

equation, Steady State performance characteristics are calculated for power law index, n=1.4, 1.5, 1.6, 1.7, 1.8, 1.9, 2 and 2.1 for Two Axial Groove bearing and the L/D ratio considered here is 1. Following results are the observations noted from the

calculated values.

For all power law index values from  $n=1.4$  to 2.1, the value of attitude angle decreases while increasing the values of eccentricity ratio as shown in Fig. 19. Similarly, for a particular eccentricity ratio, the attitude angle decreases while increasing the values of flow behaviour index from 1.4 to 2.1. Due to the increase of pressure inside the bearing on increasing the value of  $n$  and  $\epsilon$ , the load carrying capacity, which is proportional to pressure, will increase due to which attitude angle decreases.

On the other hand, for all power law index values from  $n=1.4$  to 2.1, the value of Load Carrying Capacity increases while increasing the values of eccentricity ratio as shown in Fig. 20. In addition, while keeping the eccentricity ratio constant, the values of Load Carrying Capacity increase while increasing the values of flow behaviour index 1.4 to 2.1. On increasing the value of  $n$  and  $\epsilon$  the pressure increases inside the bearing, the load carrying capacity is directly proportional to pressure. Therefore, the load carrying capacity will also increase.

The values of Sommerfeld Numbers can be observed decreasing while increasing the eccentricity ratio values keeping the value of flow behaviour index constant as shown in Fig.21.

Similarly, for a particular eccentricity ratio, the values of Sommerfeld Numbers decrease while increasing the values of flow behaviour index from 1.4 to 2.1. It is clear that sommerfeld number is inversely proportional to load carrying capacity. Therefore, as load carrying capacity increases the Sommerfeld number decreases. At a given value of eccentricity ratio, the value of friction variable decreases while increasing the flow behaviour index from 1.4 to 2.1 as shown in Fig. 22. Similarly, at a given value of power law index, the values of Friction Variable decrease while keeping the value of eccentricity ratio constant. Due to increase of lubricant pressure, it is clear that the fluid film thickness reduces. The friction variable, which is directly proportional to fluid film thickness, will also reduce. With the increase of power law index from 1.4 to 2.1, the values of flow coefficient increases for same value of eccentricity ratio as shown in Fig. 23. On keeping the power law index constant, on increasing the values of eccentricity ratio the value of Flow Coefficient increase. Flow coefficient is directly proportional to pressure. As the value of pressure inside the lubricant increases on increasing  $n$  and  $\epsilon$ , thus the value of flow coefficient also increases.

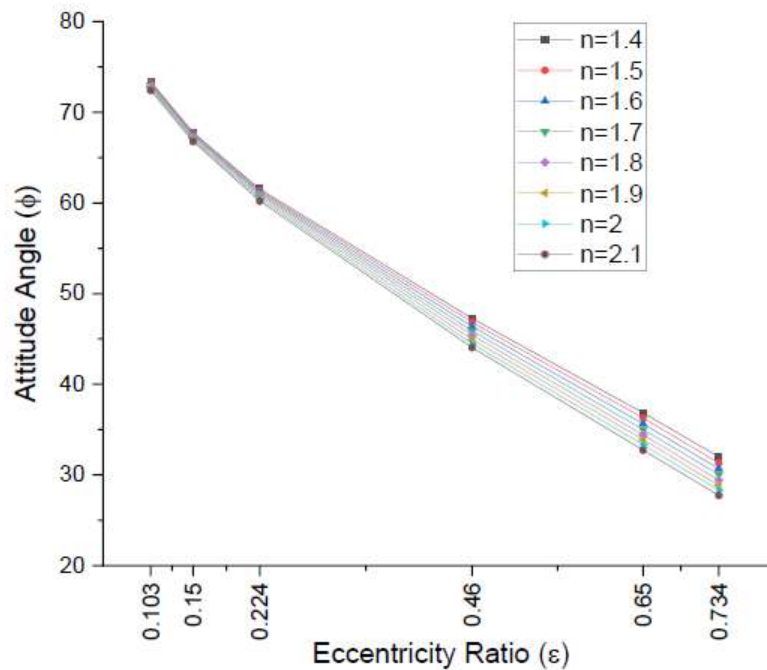


**FIGURE 19** Variation of Attitude Angle with eccentricity ratio & power law index

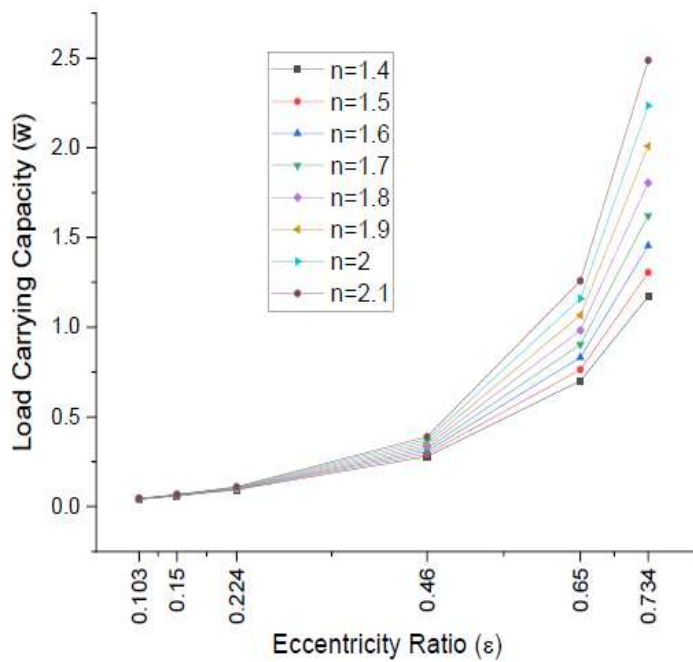


FIGURE 20 Variation of Load Capacity with eccentricity ratio & power law index

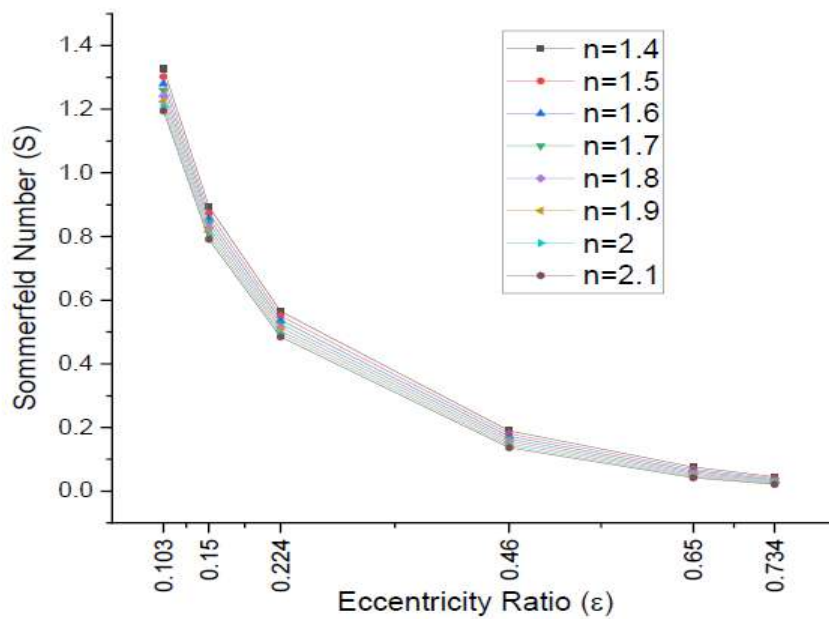


FIGURE 21 Variation of Sommerfeld No. with eccentricity ratio & power law index

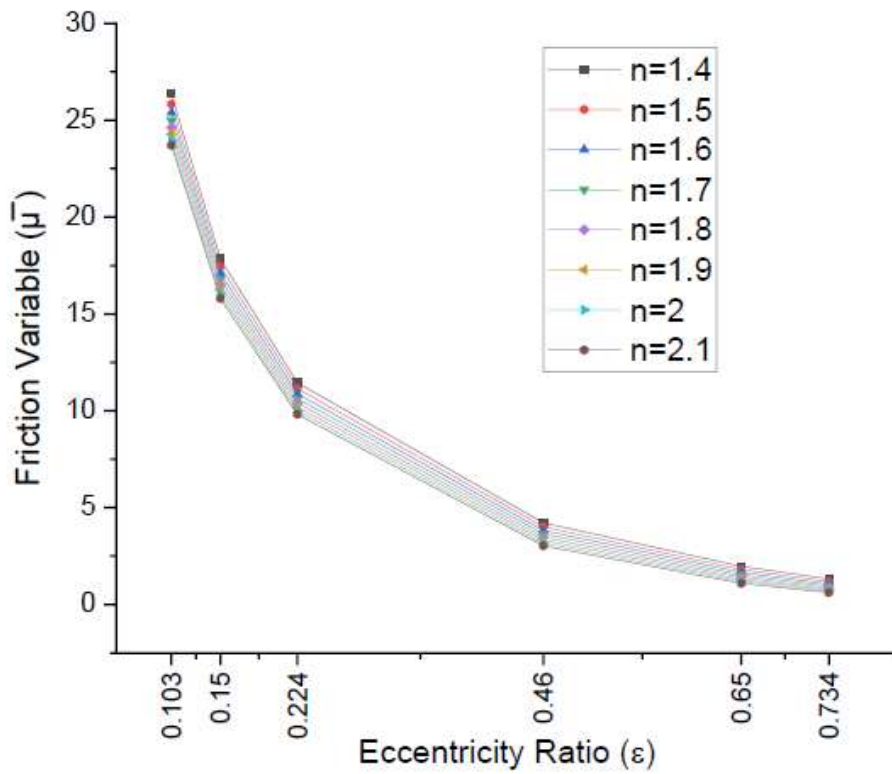


FIGURE 22 Variation of friction Coefficient with eccentricity ratio & power law index

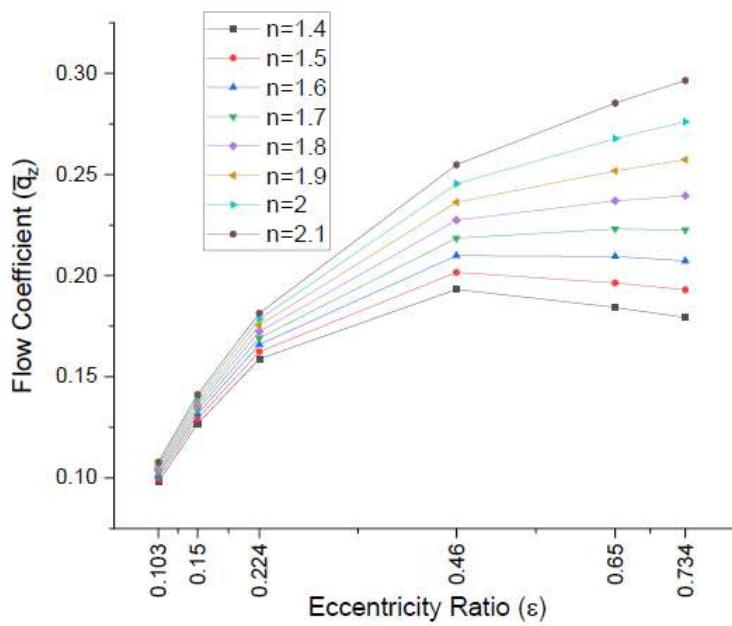


FIGURE 23 Variation of Flow Coefficient with eccentricity ratio & power law index

From the above figures, it has become clear that as the hydrodynamic pressure increases, Sommerfeld number decreases with increase of  $n$  and  $\epsilon$ . The load carrying capacity of bearing increases with the increase of  $n$  and  $\epsilon$ . Attitude angle decreases with the increase of  $n$  for same value of  $\epsilon$ . Friction variable decreases with increase of  $n$  at a given value of  $\epsilon$ . With the increase of  $n$ , flow coefficient increases with increase of  $\epsilon$ . With the increase of both  $n$  and  $\epsilon$ , pressure inside the bearing rises, which causes an increase in the flow coefficient

### Two Lobe Bearing

The steady state performance characteristics calculated for two-lobe bearing is shown in Table 2, For validation of the results, the steady state performance characteristics like Sommerfeld number and Attitude Angle obtained for Newtonian lubricant is compared with previously obtained result [48]. The small variation in results can be seen when compared with [48] may be due to setting of the more convergence criteria in the present work

**TABLE 3.** For  $L/D=1$ ,  $n=1$  validation of theoretical model for two lobe bearing

$\epsilon$	S	[48]	$\phi$	[48]
0.05	1.4663	[1.442]	93.9450	[93.9100]
0.15	0.4457	[0.442]	91.9450	[91.9700]
0.25	0.2238	[0.224]	87.9450	[88.2800]
0.35	0.1221	[0.120]	81.8450	[81.9400]
0.451	0.0457	[0.045]	83.9450	[63.7000]

### Estimation of Steady State Performance Characteristics of Two Lobe Bearing Using Non-Newtonian Fluid (Dilatant Fluid from $n=1.4$ to 2.1)

Using numerical solution of Reynolds equation, Steady State performance characteristics are calculated for power law index,  $n=1.4, 1.5, 1.6, 1.7, 1.8, 1.9, 2$  and  $2.1$  for Two lobe bearing and the  $L/D$  ratio considered here is 1. Following results are the observations noted from thecalculated values.

For all power law index values from  $n=1.4$  to  $2.1$ , the value of attitude angle decreases while increasing the values of eccentricity ratio as shown in Fig. 24. Similarly, for a particular eccentricity ratio, the attitude angle decreases while increasing the values of flow behaviour index from  $1.4$  to  $2.1$ . Due to the increase of pressure inside the bearing on increasing the value of  $n$  and  $\epsilon$ , the load carrying capacity, which is proportional to pressure, will increase due to which attitude angle decreases. On the other hand, for all power law index values from

$n=1.4$  to  $2.1$ , the value of Load Carrying Capacity increases while increasing the values of eccentricity ratio as shown in Fig. 25. In addition, while keeping the eccentricity ratio constant, the values of Load Carrying Capacity increase while increasing the values of flow behaviour index  $1.4$  to  $2.1$ . On increasing the value of  $n$  and  $\epsilon$  the pressure increases inside the bearing, from the load carrying capacity is directly proportional to pressure. Therefore, the load carrying capacity will also increase. The values of Sommerfeld Numbers can be observed decreasing while increasing the eccentricity ratio values keeping the value of flow behaviour index constant as shown in Fig.26. Similarly, for a particular eccentricity ratio, the values of Sommerfeld Numbers decrease while increasing the values of flow behaviour index from  $1.4$  to  $2.1$ . It is clear that sommerfeld number is inversely proportional to load carrying capacity. Therefore, as load carrying capacity increases the Sommerfeld number decreases.

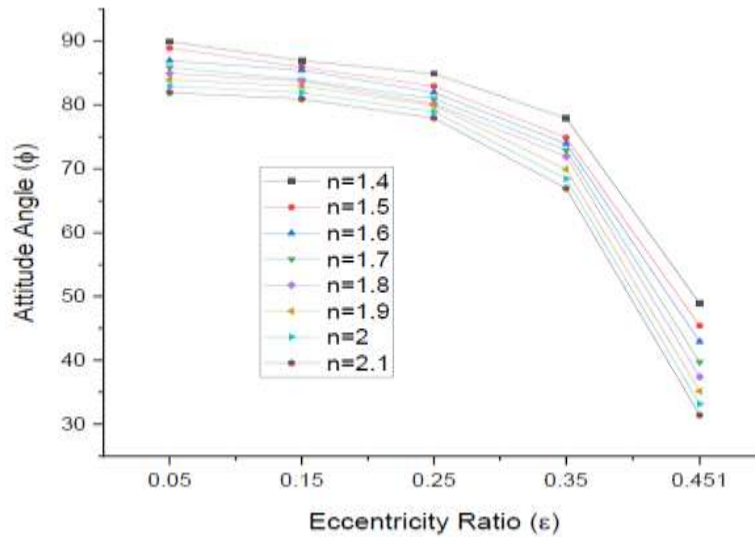


FIGURE 24 Variation of Attitude Angle with eccentricity ratio & power law index

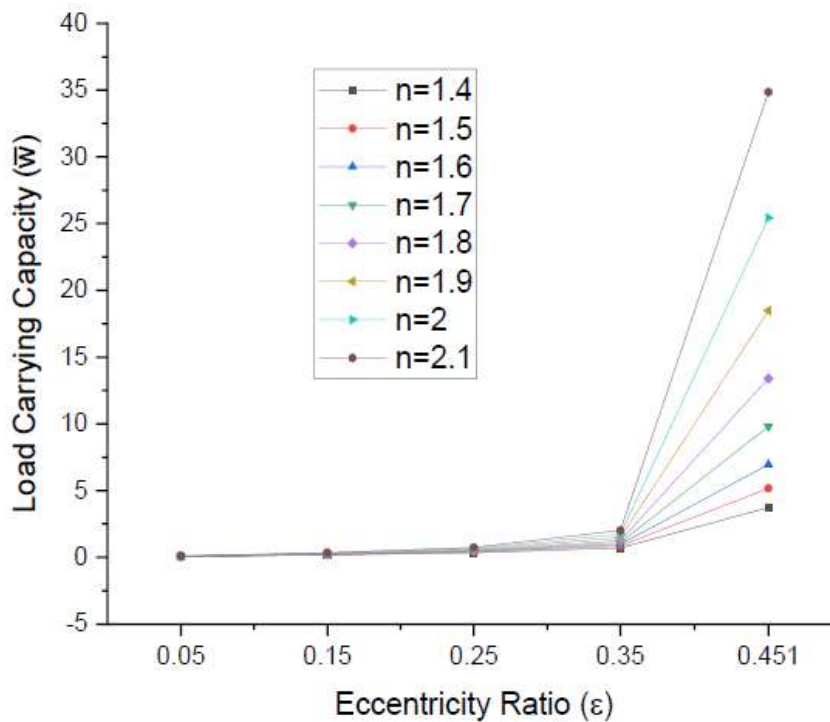


FIGURE 25 Variation of Load carrying capacity with eccentricity ratio & power law index



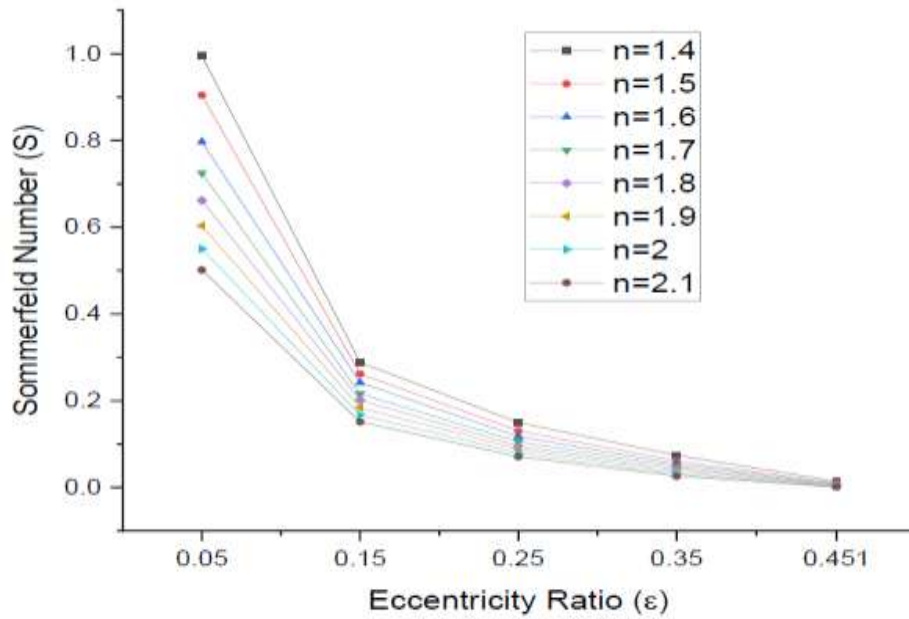


FIGURE 26 Variation of Sommerfeld Number with eccentricity ratio & power law index

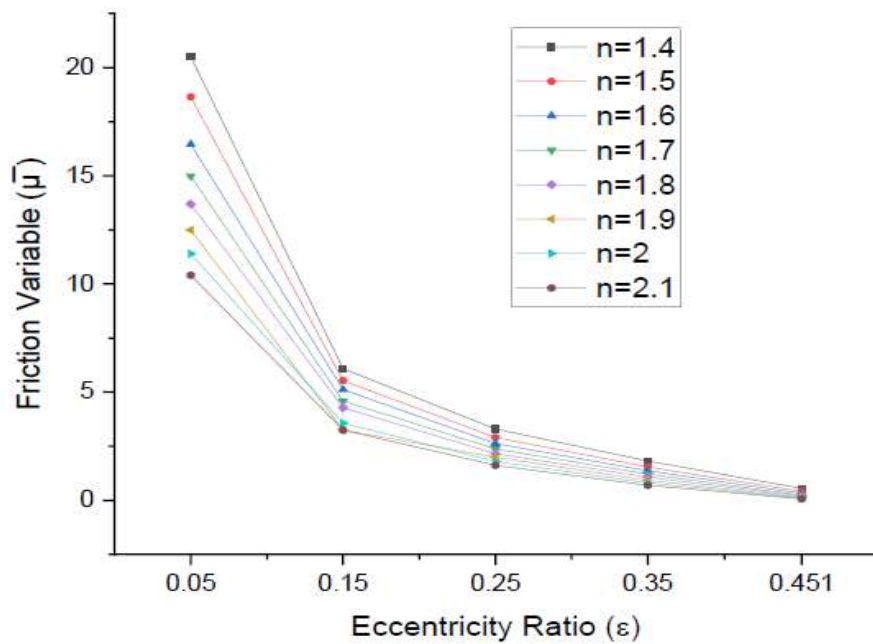
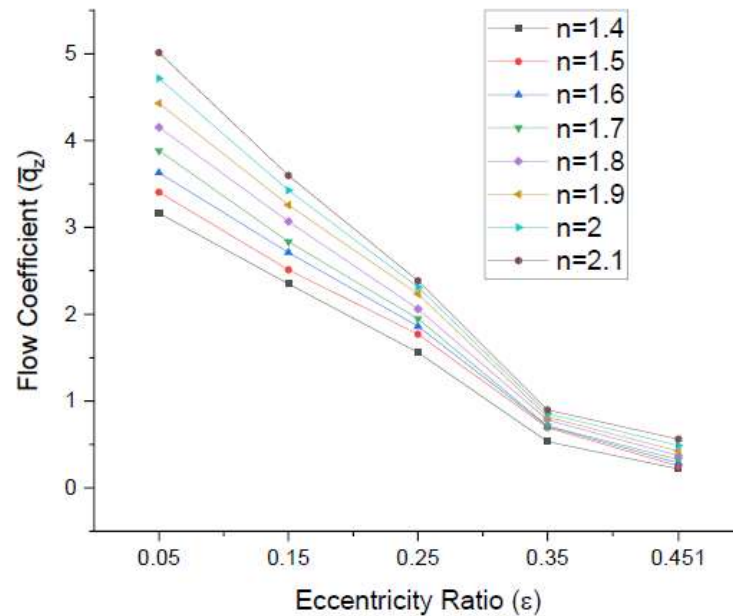


FIGURE 27 Variation of Friction Variable with eccentricity ratio & power law index



**FIGURE 28** Variation of Flow Coefficient with eccentricity ratio & power law index

At a given value of eccentricity ratio, the value of friction variable decreases while increasing the flow behaviour index from 1.4 to 2.1 as shown in Fig. 27. Similarly, at a given value of power law index, the values of Friction Variable decrease while keeping the value of eccentricity ratio constant. Due to increase of lubricant pressure, it is clear that the fluid film thickness reduces. Thus, friction variable, which is directly proportional to fluid film thickness, will also reduce.

With the increase of power law index from 1.4 to 2.1, the values of flow coefficient decreases for same value of eccentricity ratio as shown in Fig. 28. On keeping the power law index constant, on

increasing the values of eccentricity ratio the value of Flow Coefficient decrease.

### Three Lobe Bearing

The steady state performance characteristics calculated for three-lobe bearing is shown in Table 4. For validation of the results, the steady state performance characteristics like Sommerfeld number and Attitude Angle obtained for Newtonian lubricant is compared with previously obtained results [48]. The small variation in results can be seen when compared with [48] may be due to setting of the more convergence criteria in the present work.

**TABLE 4** For L/D=1, n=1 validation of theoretical model for three lobe bearing

ε	S [48]	Ø [48]
0.103	0.4352 [0.5740]	43.8900 [60.9500]
0.203	0.2269 [0.2450]	56.9450 [60.4400]
0.285	0.1346 [0.1380]	56.8900 [58.2200]
0.351	0.0841 [0.0850]	54.4450 [55.2300]
0.441	0.0321 [0.0340]	44.9450 [47.1900]

### Estimation of Steady State Performance Characteristics of Three Lobe Bearing Using Non-Newtonian Fluid (Dilatant Fluid from n=1.4 to 2.1)

One of the most extensively used multi-

lobe bearing is three lobe bearing as it can sustain more load capacity. In this work asymmetric three lobe bearing having 70 degree lobe each and 20 degree groove angle. Considering L/D =1, steady state performance characteristics are obtained for

power index ( $n$ ) = 1.4, 1.5, 1.6, 1.7, 1.8, 1.9, 2 and 2.1

For a given eccentricity ratio ( $\epsilon$ ), with the increase of power law index, the Attitude angle ( $\phi$ ) starts increasing at first and then decreasing. Also, Attitude angle increases and then decreases with the increase of eccentricity ratio for a given power law index as shown in Fig. 29. Load capacity increases with increase of power index ( $n$ ) for a given eccentricity ratio ( $\epsilon$ ) and for a given power index, the load capacity increases with the increase of eccentricity ratio as shown in Fig. 30. For a given eccentricity ratio ( $\epsilon$ ), Sommerfeld number ( $S$ ) decreases with increase of power law index ( $n$ ) and

Sommerfeld number decreases with the increase of eccentricity ratio for a given power law index as shown in Fig. 31. At a certain value of eccentricity ratio ( $\epsilon$ ) friction variable ( $\bar{\mu}$ ) decreases with the increase of power law index ( $n$ ) as shown in Fig. 32. With the increase of eccentricity ratio friction variable decreases for a particular value of power law index. With the increase of power law index ( $n$ ) flow coefficient ( $\bar{q}$ ) increases then decreases for the same value of eccentricity ratio ( $\epsilon$ ) as shown in Fig. 33 and for a particular value of power law index, with the increase of eccentricity ratio, flow coefficient first slightly increases then decreases.

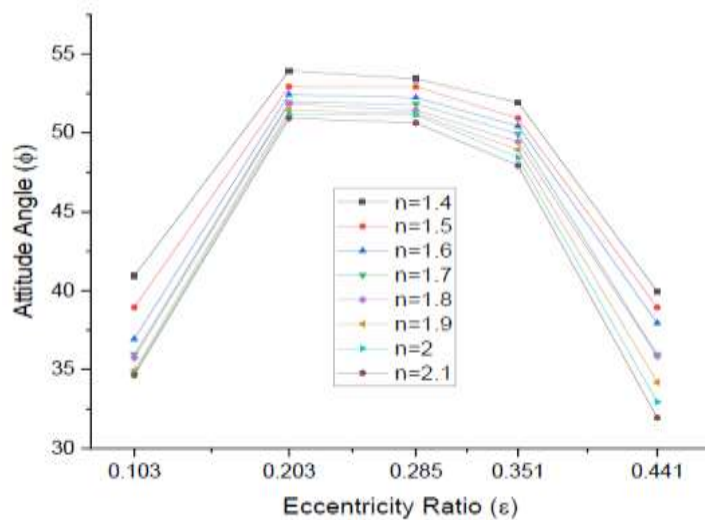


FIGURE 29 Variation of Attitude Angle with eccentricity ratio & power law index

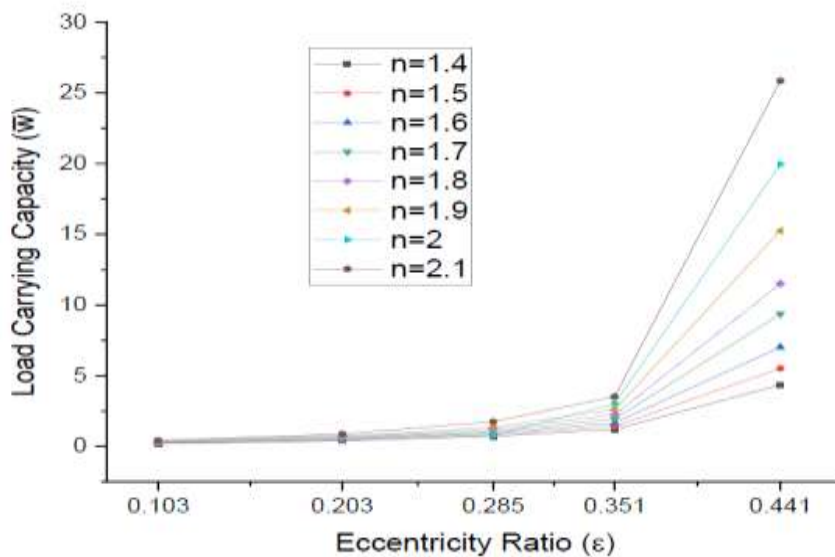


FIGURE 30 Variation of Load carrying capacity with eccentricity ratio & power law index

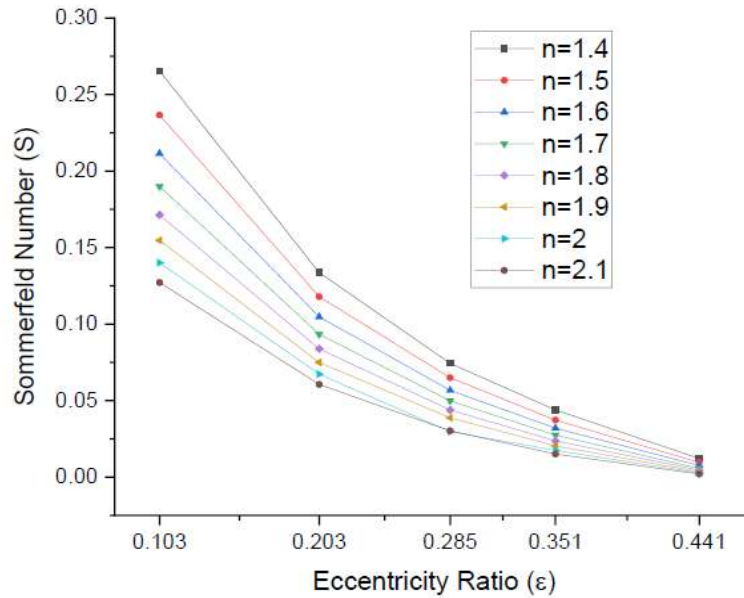


FIGURE 31 Variation of Sommerfeld number with eccentricity ratio & power law index

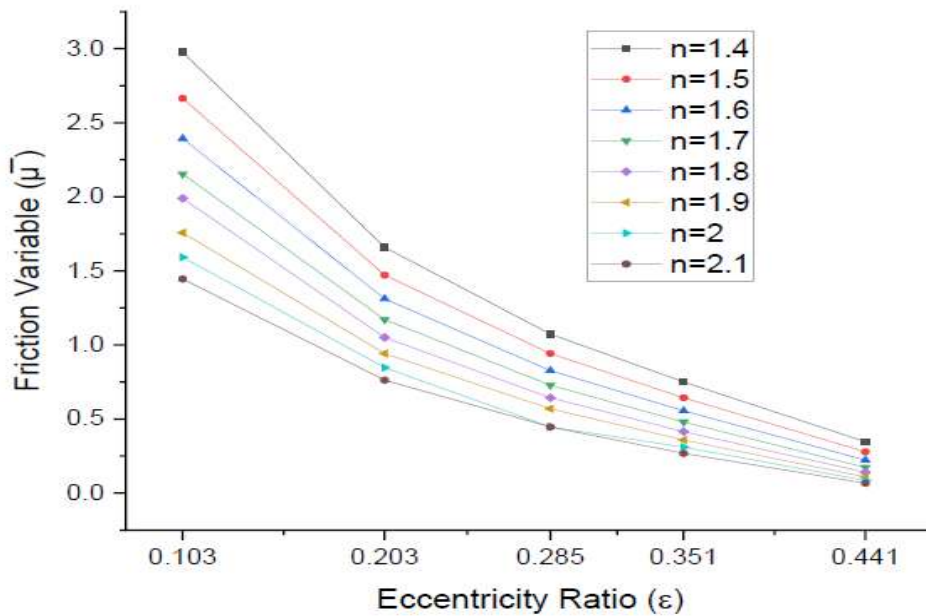


FIGURE 32 Variation of Friction variable with eccentricity ratio & power law index

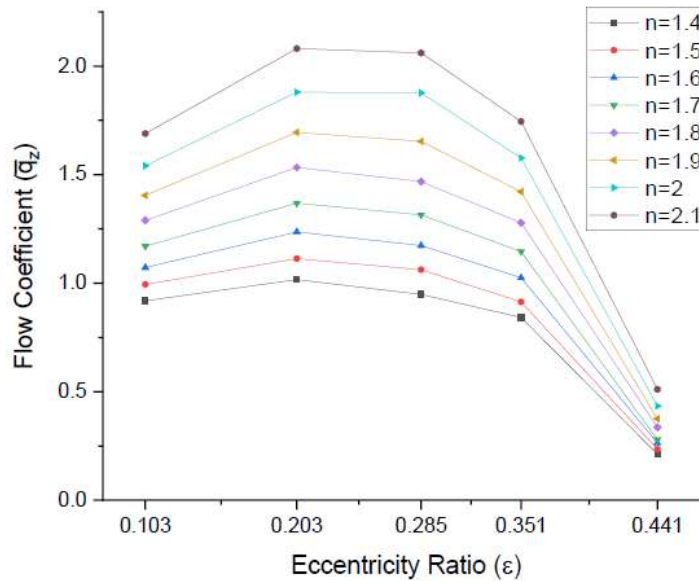


FIGURE 33 Variation of Flow coefficient with eccentricity ratio & power law index

**Four Lobe Bearing**

The steady state performance characteristics are calculated for four-lobe bearing using Newtonian lubricant having 10-degree groove angle as shown in Table 5 and validated

with previously obtained results [48]. From Fig. 34, Fig.35, Fig. 36, Fig. 37 and Fig. 38, it is clearly seen the effect of power law index and eccentricity ratio on steady state performance characteristics for four lobe bearing having 20 degree groove angle.

TABLE 5 For L/D=1, n=1 validation of theoretical model for three lobe bearing

epsilon	S [48]	Ø [48]
0.203	0.3238 [0.2230]	54.9450 [51.2300]
0.285	0.1705 [0.1620]	51.9450 [47.8000]
0.351	0.0970 [0.0870]	48.9450 [42.0000]
0.375	0.0752 [0.0660]	45.9450 [40.0000]

**Estimation of Steady State Performance Characteristics of Four Lobe Bearing Using Non-Newtonian Fluid (Dilatant Fluid from n=1.4 to 2.1)**

A non-circular bearing consists of four lobe where each lobe having different centres of curvature moved toward the bearing centre. In this work four 20 degree groove angle is used which are perpendicular to the horizontal axis.

Attitude angle (Ø) decreases with the increase of power index (n) at a particular eccentricity ratio (epsilon) as shown in Fig. 34. For a certain value of power index, attitude angle decreases with increase of eccentricity ratio. At particular eccentricity ratio (epsilon) load carrying

capacity (W) increases with the increase of power law index (n) and at a given power law index load carrying capacity increases with the increase of eccentricity ratio as shown in Fig. 35 . It is seen that at higher eccentricity ratio load carrying capacity increases more for increase of power law index.

Sommerfeld number (S) decreases with the increase of power law index (n) value of eccentricity ratio (epsilon) and at a particular power index Sommerfeld number decreases with the increase of eccentricity ratio as shown in Fig. 36.

At a given value of eccentricity ratio (epsilon) friction variable (mu) decreases with increase of power index (n) as shown in Fig. 37. With increase of eccentricity ratio, friction variable decreases for particular value of power law index.

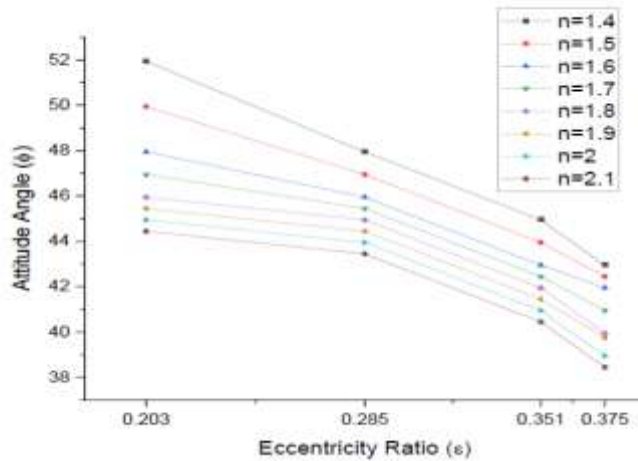


FIGURE 34 Variation of Attitude Angle with eccentricity ratio & power law index

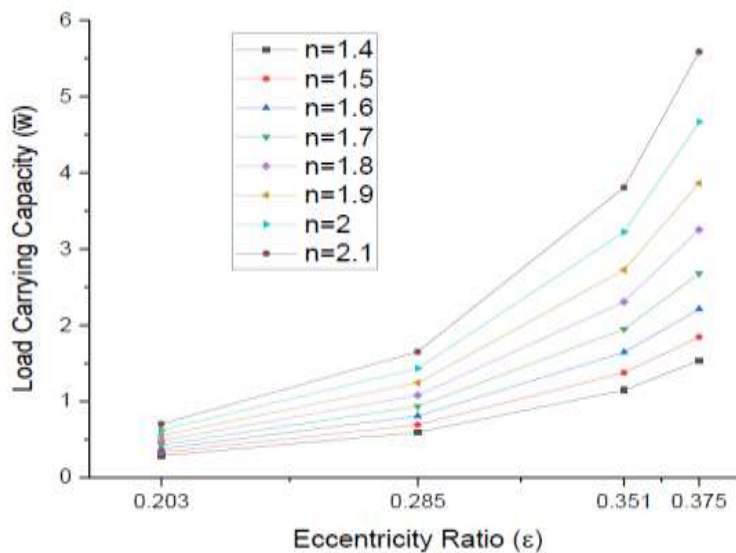


FIGURE 35 Variation of Load carrying capacity with eccentricity ratio & power law index

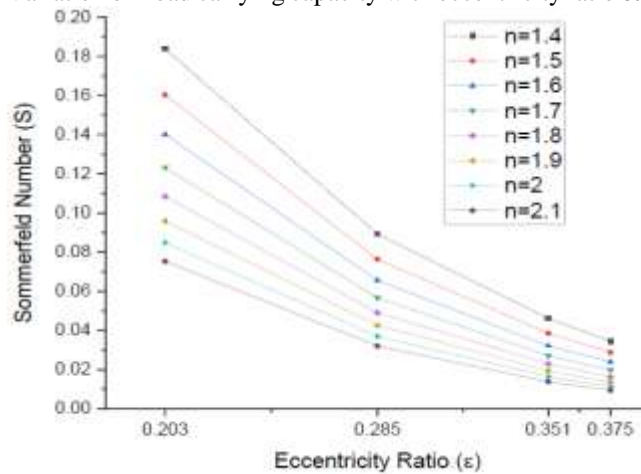


FIGURE 36 Variation of Sommerfeld number with eccentricity ratio & power law index

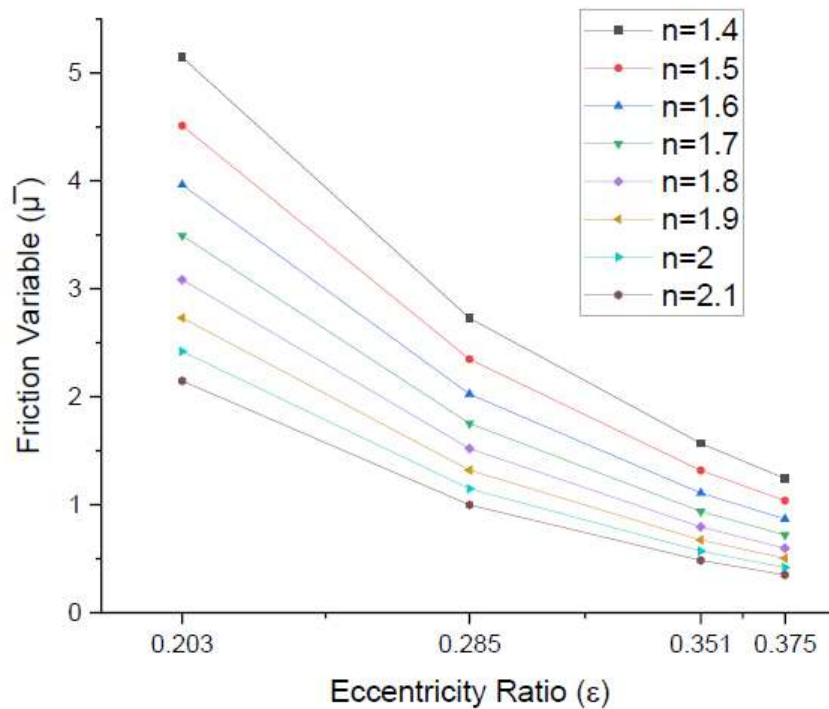


FIGURE 37 Variation of Friction variable with eccentricity ratio & power law index

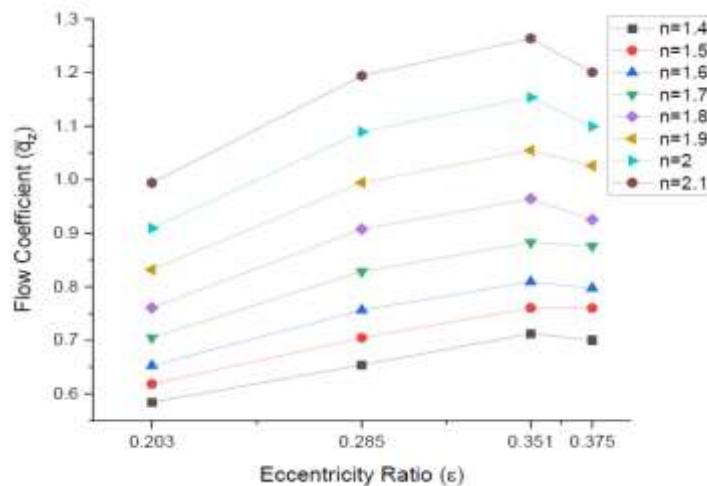


FIGURE 38 Variation of Flow coefficient with eccentricity ratio & power law index

At a particular eccentricity ratio ( $\epsilon$ ) flow coefficient ( $\bar{q}$ ) increases at first and finally decreases with the increase of power law index ( $n$ ) as shown in Fig.39. With increase of eccentricity, ratio flow coefficient increases at first and then slightly decreases

**Extent of Power Law Index (n) up to Which Dilatancy Exists**

We know that, Friction Coefficient

It can be observed that Friction Variable ( $\bar{\mu}$ ) is inversely proportional to Viscosity of the lubricant ( $\eta$ ). We have seen from that the value of friction variable decreases as the viscosity of the dilatant fluid increases with increasing value of flow behaviour index ( $n$ ). Dilatant fluids are also known as shear-thickening fluid. The viscosity of these fluids will increase as the shear rate increases. However, at a certain flow behaviour index value, it has been observed that the friction variable starts

increasing which means after the particular amount of flow behaviour index ( $n$ ), the viscosity of the fluid starts decreasing. In order to find the extent of flow behaviour index up to which dilatancy exists various values of  $n$  are inserted as input and for various eccentricity ratios the values of friction variables are found for plain cylindrical bearing.

From this experiment, it has been found that up to flow behaviour index ( $n$ ) equal to 125, the

values of friction variable decreases i.e. the value of viscosity increases, which is a property of dilatant fluid. However, at value of flow behaviour index 126, the friction variable for two different eccentricity ratio values 0.103 and 0.150 are observed as the same. In addition, while increasing the value of eccentricity ratio, the friction variables can be seen further increasing as shown in Fig. 39.

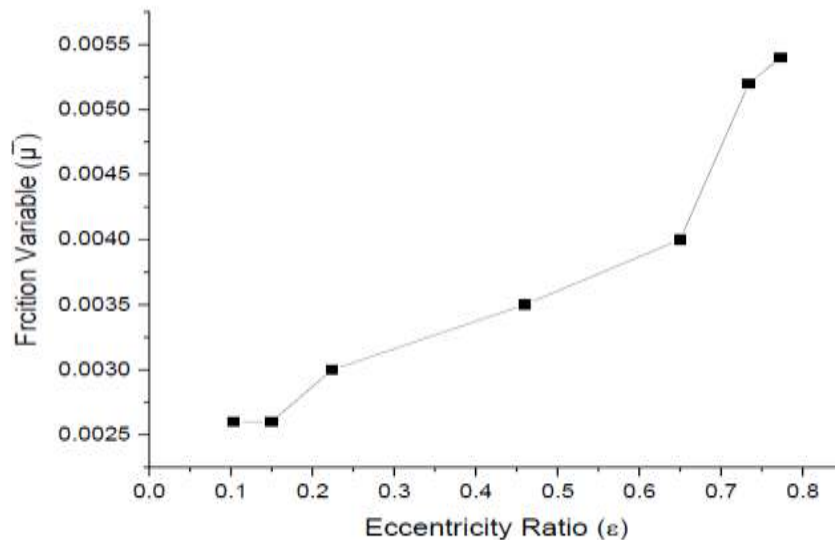


**FIGURE 39** Variation of friction variable with eccentricity ratio at power law index 126

From this it is clear that after the value of flow behaviour index 125 the value of viscosity decreases with increasing the shear rate. Therefore, dilatancy exists for flow behaviour index value 125 and from 126, the dilatancy property does not exist

## II. CONCLUSION

A computational analysis of steady state performance characteristics have been carried out on plain cylindrical bearing, two axial groove bearing and multi-lobe bearing using non-Newtonian (Dilatant) lubricant in this work. The influence of different eccentricity ratios and power law index of non-Newtonian lubricant on steady state performance characteristics of plain cylindrical bearing, two axial groove bearing and multi-lobe bearing has been discussed and compared the results with results obtained using Newtonian lubricants. The following conclusions are evident from the study.

- Increase of power law index causes increase in pressure, which leads to increase in non-dimensional load carrying capacity at a

particular eccentricity ratio.

- As non-dimensional load, capacity is inversely proportional to Sommerfeld number and attitude angle, with the increase of power index, Sommerfeld number and attitude angle decreases at a particular eccentricity ratio for most the bearing configurations. Only in three-lobe bearing, a slight increase in attitude angle can be observed with the increase of power law index. But, finally attitude angle can be seen decreasing with increasing power law index.
- As viscosity and load carrying capacity increases with increase in power index leads to decrease in friction variable for all types of bearing configurations. For multi-lobe bearing, it is observed that the friction variable is lesser than plain cylindrical bearing and two axial groove bearing.
- Increase of power index causes rise in pressure, which lead to increase in radial clearance results in increase of flow coefficient in plain cylindrical bearing, two axial groove bearing and four-lobe bearing. It is better to have higher flow coefficient because oil



removes most of the frictional heat and cools the bearing.

- With the increase of eccentricity pressure increases inside the bearing, which leads to increase in non-dimensional load carrying capacity at a particular power law index value.
- With the increase of eccentricity ratio, Sommerfeld number and attitude angle, which are inversely proportional to non-dimensional load carrying capacity, decrease at a constant value of power law index value.
- For dilatant fluid as lubricant, It has been found that among all types of bearing configuration, two-lobe bearing shows appreciably more load carrying capacity.

#### REFERENCES

- [1]. Chauhan, A., Sehgal, R., Sharma, R.K., 2011, "Investigations on the thermal effects in non-circular journal bearing", *Tribology International*, Vol. 44, pp. 1765-73.
- [2]. P.D. William, G.R. Symmons., 1987., "Analysis of Hydrodynamic Journal Bearings Lubricated with Non-Newtonian fluids", *Tribology International*, 20(3), pp.119-124.
- [3]. O. Reynolds, "On the Theory of Lubrication and Its Application to Mr. Beauchamp Tower's Experiments, Including an Experimental Determination of the Viscosity of Olive Oil," *Philosophical Transactions of the Royal Society of London*, vol. 177, pp. 157-234, 1886.
- [4]. Reynolds O., 1886, "On the Theory and Lubrication and its Application to Mr. Beauchamp Tower's Experiments including an Experimental Determination of Viscosity of Olive Oil," *Phil. Trans. Royal Soc. Naval Engrs.*, Vol. 9, pp. 267-292.
- [5]. B. Tower, "First Report on Friction Experiments," *Proceedings of Institution of Mechanical Engineers*, pp. 632-659, 1883.
- [6]. A Sommerfeld, "Zur Hydrodynamische Theorie der Schmiermittelreibung," *Zeitschrift für angewandte Mathematik und Physik*, vol. 50, pp. 97-155, 1904
- [7]. B. Jacobson and L. Floberg, "The finite journal bearing considering vaporization," *Trans. Chalmers. Univ. Tech. Gothenburg*, pp. 189-190, 1957.
- [8]. G. DuBois and F. Ocvirk, "Analytical derivation and experimental evaluation of short-bearing approximation for full journal bearing," *NACA Report*, vol. 1157, 1953.
- [9]. Reyleigh, Lord, 1918, "Notes on Theory of Lubrication," *Phil. Mag.*, vol. 53, pp.112.
- [10]. Shaw, M. C. and Macks, E. F., 1949, "Analysis and Lubrication of Bearing," *McGrawHill Book Co.*
- [11]. Ocvirk, F. W., 1952, "Short Bearing Approximation for Full Journal Bearing," *NACA, TN 2808*.
- [12]. Pinkus, O., 1958, "Solution of Reynolds equation for finite journal bearing", *Trans. ASME*, vol. 80, pp. 858-864.
- [13]. Raimondi, A. A., and Boyd, J., 1958, "A Solution for the Finite Journal Bearing and Its Application to Analysis and Design", I, II and III, *ASLE Trans*, vol. 1, pp. 159-209.
- [14]. Knight, J. D., Barrett L. E., and Cronan R. D., 1984, "Effect of Supply Pressure on the Operating Characteristics of Two-Axial-Groove Journal Bearings," *ASLE Trans.*, vol. 28, pp. 336-342.
- [15]. ESDU Items 84031 (and 85028), *Calculation Methods for Steadily Loaded Axial Groove Hydrodynamic Journal Bearings, with super laminar operation*, December 1985, 1984.
- [16]. P. Klit and J. W. Lund, "Calculation of the dynamic coefficients of a journal bearing, using a variational approach," *Journal of Tribology*, vol. 108, no. 3, pp. 421-425, 1986.
- [17]. D. T. Gethin and M. K. I. El Deihi, "Effect of loading direction on the performance of a twin-axial groove cylindrical bore bearing," *Tribology International*, vol. 20, no. 4, pp. 179-185, 1987.
- [18]. Akkok, M., and Ettles, C. M. McC., 1979, "The Effect of Grooving and Bore Shape on the Stability of Journal Bearings," *ASLE Trans.*, vol. 23, 4, pp. 397-403
- [19]. Wilcock, Donald F., 1987, "Influence of Feed Groove Pressure and Related Flow on Journal Bearing Performance," *STLE Tribology Trans.*, vol. 31, 3, pp. 397-403.
- [20]. Pinkus, O., 1956, "Analysis of Elliptical Bearings," *Trans. ASME*, 78, pp. 965-973.
- [21]. Pinkus, O., 1959, "Analysis and Characteristics of Three-Lobe Bearings,"

- Trans. ASME, J. Basic Eng., 81, pp. 49-55.
- [22]. Lund, J. W., 1965, "Rotor-Bearing Dynamics Design Technology, Part III: Design Handbook for Fluid-Film Type Bearings," Mechanical Technology, Technical Report No. AFAPL-TR-65-45.
- [23]. Lund, J. W., 1968, "Rotor-Bearing Dynamics Design Technology, Part VII: The Three-Lobe Bearing and Floating Ring Bearing," Mechanical Technology, Technical Report No. AFAPL-TR-65-45.
- [24]. Lund, J. W., and Thomsen, K. K., 1978, "A Calculation Method and Data for the Dynamic Coefficients of Oil-Lubricated Journal Bearings." Topics in Fluid Film Bearing and Rotor Bearings System Design and Optimization, The ASME Design Engineering Conference, pp. 1-29.
- [25]. Shang, L., and Dien, L. K., 1989, "A Matrix Method for Computing the Stiffness and Damping Coefficients of Multi-Arc Journal Bearing," Tribol. Trans., 32(3), pp. 396-404.
- [26]. Gian Bhushan, S. S. Rattan and N. P. Mehta (2002) "Stability analysis of four-lobe pressure-dam bearings." Tribology Letters, vol. 13, No. 1.
- [27]. Glienicke, J., Han, D. C., and Leonhard, M., 1980, "Practical Determination and Use of Bearing Dynamic Coefficients," Trib. Int., 13(6), pp. 297-309.
- [28]. Someya, T., 1989, Journal Bearing Design Data Book, Springer, Berlin.
- [29]. R. D. Flack, M.E. Leader, and P.E. Allaire, "An experimental and theoretical investigation of pressure in four lobe bearings" Wear, vol. 61, 1980, pp. 223-242
- [30]. Knight, J. D., and Barrett, L. E., 1983, "A Approximate Solution Technique for Multi-Lobe Journal Bearing Including Thermal Effects, With Comparison to Experiment," ASME Trans., 26(4), pp. 501-508.
- [31]. P. D. William, G. R. Symmons, 1987, "Analysis of Hydrodynamic Journal Bearings Lubricated with non-Newtonian fluids," Tribology International, 20(3), pp. 287-295.
- [32]. E. Dean and G. Davis, "Viscosity Variations of Oils With Temperature," Chem. And Met. Eng., vol. 36, pp. 618-619, 1929.
- [33]. R. Haycock, A. J. Caines, R. F. Haycock and J. E. Hillier, Automotive Lubricants Reference Book, John Wiley and Sons, 2004.
- [34]. D. Oliver, "Load enhancement effects due to polymer thickening in a short model journal bearing," Journal of non-Newtonian Fluid Mechanics, vol. 30, no. 2-3, pp. 185-196, 1988.
- [35]. F. Dai and M. Khonsari, "On the solution of a lubrication problem with particular solids," International Journal of Engineering Science, vol. 29, no.9, pp. 1019-1033, 1991.
- [36]. F. Dai and M. Khonsari, "Analytical solution for a mixture of a Newtonian fluid and granules in hydrodynamic bearings," Wear, vol. 156, no. 2, pp. 327-344, 1992
- [37]. G. Maiti, "Micropolar Squeeze Film Bearing," Japanese Journal of Applied Physics, vol. 13, no. 9, pp. 1440-1442, 1974.
- [38]. M. Khonsari and D. Brewe, "On the performance of finite journal bearings lubricated with micropolar fluids," STLE Tribology Transactions, vol. 32, no. 2, pp. 155-160, 1989.
- [39]. Hsu Y. C. Non-Newtonian flow in infinite length full journal bearing. Trans ASME, J of Lubrication Technology, 1967, 89: 329-33.
- [40]. Swamy STN, Prabhu BS , Rao BVA. Calculated load capacity of non-Newtonian lubricants in finite width journal bearings. Wear 1975; 31: 277-85.
- [41]. Swamy STN, Prabhu BS , Rao BVA. Stiffness and damping characteristics of finite width journal bearings with non-Newtonian film and their application to instability prediction. Wear 1975; 32(3): 379-90.
- [42]. Swamy STN, Prabhu BS , Rao BVA. Steady state and stability characteristics of a hydrodynamic journal bearing with a non-Newtonian lubricant. Wear 1977; 42(2):229-44.
- [43]. Tayal S. P., Sinhasan R, Singh D. V. Static analysis of hydrodynamic journal bearing having non-Newtonian lubricants by finite element method. Third ISME Conference on Mechanical Engineering, IIT Delhi, India, 1982, pp. 245-50
- [44]. Ashutosh Kumar, Sashindra K Kakoty., Effect of couple-stress parameter on the steady state performance parameters of

- two-lobe journal bearing operating with Non-Newtonian lubricant”.
- [45]. Abdessamed Nessim, Salah Larbi, Hacene Belhaneche, and Maamar Malki., “Journal Bearings Lubrication Aspect Analysis Using Non-Newtonian Fluids”.
- [46]. Reynolds O., 1886, “On the Theory and Lubrication and its Application to Mr. Beauchampx Tower’s Experiments including an Experimental Determination of Viscosity of Olive Oil,” Phil. Trans, Royal SOC., London, vol. 9, pp. 157-234.
- [47]. B.C. Majumdar., “Introduction to Tribology of bearings” ..
- [48]. Lund W, Thomson K. K., “A Calculation Method and Data for the Dynamic Coefficients of Oil Lubricated Journal Bearings”, 1978, Proceedings of the ASME Design and Engineering Conference, Minneapolis, pp. 1-28